Exploitation of microwave sounder/imager data over land surfaces in the presence of clouds and precipitation

SAF-HYDROLOGY, Final Report

By Fatima KARBOU[1], Peter BAUER[2], Alan GEER[2] and William BELL[2]

[1] *CNRM/GAME, Météo-France and CNRS, France*
[2] *European Centre for Medium-Range Weather Forecasts, UK*

Abstract

Observations from SSMI/S are still not as intensively used in NWP as are observations from other microwave sensors. Despite their large information content, these observations are still insufficiently used. Some feasibility studies have been conducted within the ECMWF assimilation system as preliminary steps to use SSMI/S observations over land and under cloudy/rainy situations. New developments have been made in order to improve the land surface emissivity description at SSMI/S frequencies and within the constraints of 4D-VAR. Land surface emissivities have been calculated at all SSMI/S window channels and have been found in very good agreement with land surface emissivities calculated using SSM/I, AMSR-E and TMI observations. The consistency of SSMI/S emissivities has been checked by examining the variability of emissivity in space and in frequency. The land emissivity comparison has been found very helpful to check the calibration of SSMI/S window channels. Then, SSMI/S temperature and humidity sounding Tbs have been simulated using the RTTOV-SCAT model over sea and over land. The land emissivities directly retrieved at the closest (in frequency) window channel have been given to the sounding channels. We have shown that the performances of the observation operator under cloudy situations are as good over land as they are over sea. This result is very important since good Tbs simulations are necessary to make SSMI/S assimilation experiments.

[1]Email: fatima.karbou@meteo.fr

1 The project objectives

The assimilation of microwave observations in Numerical Weather Prediction (NWP) is still far from being optimal. Observations receiving a significant amount of signal from the surface as well as observations in areas of heavy clouds/rain are rejected from the assimilation systems. It is thought that to develop the use of microwave observations over land and under clear/cloudy conditions will improve the humidity analysis and the precipitation forecasts over land. Work is now carried out in many NWP centres to improve the assimilation of microwave observations under clear and cloudy situations. The assimilation of cloud affected SSM/I observations has been operational at ECMWF since June 2005 ((1), (2)). Such an accomplishment has been made possible when a two-step method (1D+4D-Var) has been adopted to assimilate a selection of SSM/I observations over sea and under cloudy situations. Cloudy SSM/I radiances are firstly assimilated within the 1D-VAR to derive Total Column Water Vapour (TCWV). The derived TCWV data are then fed to the 4D-VAR as pseudo-observations. Moreover, work got underway to assimilate Special Sensor Microwave Imager/Sounder (SSMI/S) cloudy observations over land using the 1D+4D-VAR approach (8). The main objective of this work is to investigate the feasibility of assimilating a selection of SSMI/S sounding channels over land and in cloudy situations in the 4D-VAR framework. The land surface contribution to the measured SSMI/S radiances will be estimated using land emissivities dynamically retrieved at the closest surface channel (in frequency). This method has been successfully used to assimilate AMSU-A, AMSU-B and SSMI/S over land and in clear sky situations ((13),(14)).

2 Observations and method

2.1 Microwave observations

The Special Sensor Microwave Imager/Sounder (SSMI/S) sensor is carried on two generations of the Defense Meteorological Satellite Program (DMSP) (F-16, F-17). The sensor provides unprecedented observations of the atmospheric temperature and humidity using a conical scanning technique. The SSMI/S sensor represents a huge improvement over its predecessor, the Special Sensor Microwave Imager (SSM/I), as it combines the SSM/I imaging and the profiling capabilities of ancillary microwave sounders such as the advanced microwave sounding unit (AMSU). Figure 1 shows weighting functions for a standard atmosphere and for a selection of SSMI/S chan-

nels. SSMI/S makes measurements at 24 frequencies; 14 of them are located in the 50-60 GHz range which allow atmospheric temperature sensing from about 80 Km down to the earth surface. Due to the Earth magnetic field, some of these channels are significantly affected by the Zeeman splitting effect. In addition to temperature sounding channels, SSMI/S measures humidity thanks to frequencies close to the strong 183 GHz water vapour line. Moreover, SSMI/S has 7 imaging channels in common with SSM/I. More details about the general characteristics of SSMI/S channels are presented in Table 1.

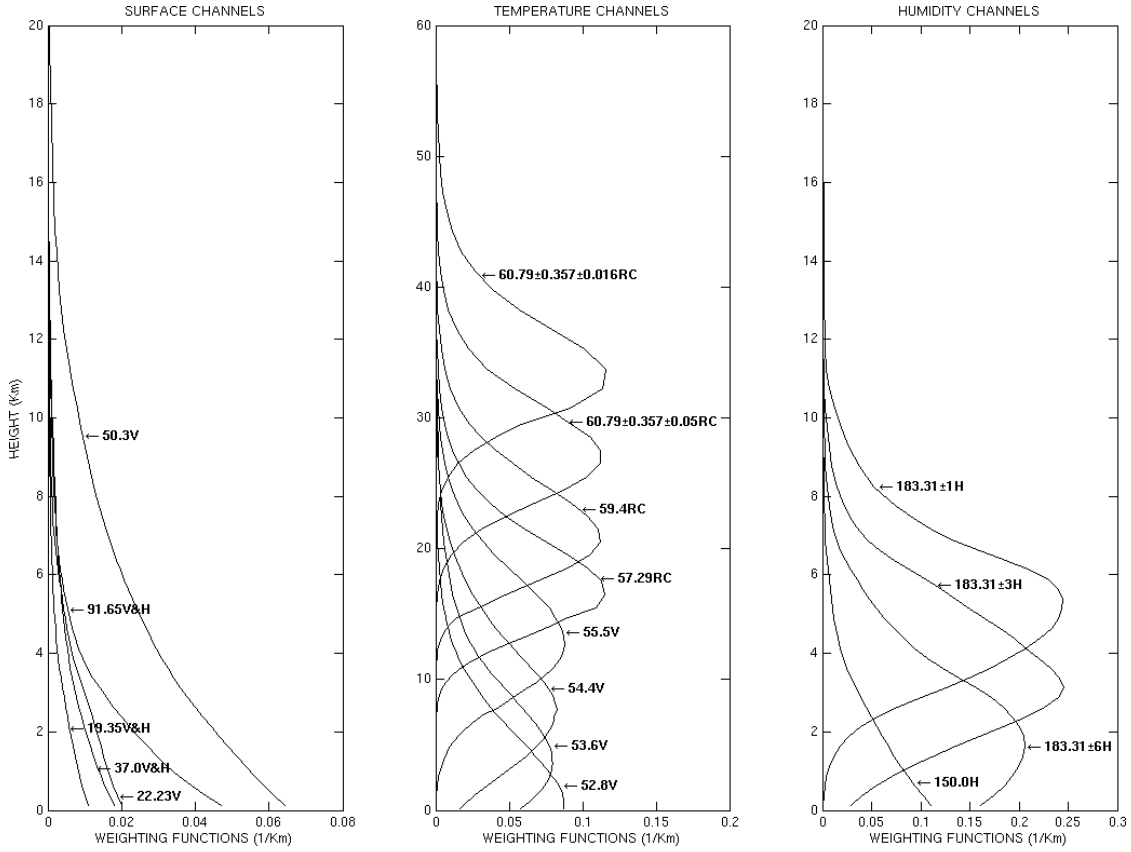

Figure 1: Weighting functions for a selection of SSMI/S channels and for a standard atmosphere.

To date, the information content of SSMI/S observations is not as intensively used in NWP as is the information content of observations from other microwave sensors. In fact, SSMI/S radiances were subject to local biases related to thermal

emission from the main reflector and to solar intrusions into the warm calibration targets. These effects have been intensively studied and calibration correction and flagging schemes have been developed to reduce the instrumental biases ((4), (23)). The assimilation of pre-processed SSMI/S observations has shown promising results (3).

Table 1: SSMI/S characteristics

Channel	Frequency (GHz)	polarisation	Sensitivity
1	50.3	V	surface
2	52.8	V	temperature
3	53.596	V	temperature
4	54.4	V	temperature
5	55.5	V	temperature
6	57.29	RC	temperature
7	59.4	RC	temperature
8	150.0	H	humidity
9	183.31±6.6	H	humidity
10	183.31±3.0	H	humidity
11	183.31±1.0	H	humidity
12	19.35	H	surface
13	19.35	V	surface
14	22.235	V	surface
15	37.0	H	surface
16	37.0	V	surface
17	91.65	V	surface+humidity
18	91.65	H	surface+humidity
19	63.28±	RC	temperature
20	$\nu = 60.79\pm$	RC	temperature
21	$\nu \pm 0.002$	RC	temperature
22	$\nu \pm 0.005$	RC	temperature
23	$\nu \pm 0.016$	RC	temperature
24	$\nu \pm 0.050$	RC	temperature

It is worthy to mention that similar instrumental biases have also been observed while processing observations from other conical scanning instruments such as the Tropical Rainfall Measurement Mission Microwave Imager (TRMM), Microwave Imager (TMI), the Advanced Microwave Scanning Radiometer - ADEOS II (AMSR),

and from SSM/I. Calibration studies have been undertaken in order to use efficaciously observations for atmospheric applications. In this study, SSMI/S observations from F-16 have been used together with observations from many other sensors. A brief description of these sensors is given in the following.
The SSM/I is a conical scanning passive microwave imager and is onboard the latest generation of the DMSP satellites since June 1987. It allows observation acquisition at four frequencies (19.3, 22.2, 37.0 and 85.5 GHz), with a dual polarization (only horizontal at 22.2 GHz) and has a near constant zenith angle of 53^o. The instrument makes measurements with a mean altitude of 830 km, a swath width of 1400 km and a horizontal resolution that varies from 12.5 km (at 85.5 GHz) to 25 km (at 19.3 GHz). In addition to SSM/I observations, data from other microwave instruments have been used (AMSRE, TMI). The Advanced Microwave Scanning Radiometer - Earth Observing System (AMSR-E) instrument is operating aboard NASA's Aqua Satellite since 4 May 2002. It is a twelve-channel, six-frequency, passive-microwave radiometer system with a near constant zenith angle of about 55^o. It measures horizontally and vertically polarized brightness temperatures at 6.9, 10.7, 18.7, 23.8, 36.5, and 89.0 GHz. At an altitude of 705 km, AMSRE measures the upwelling scene brightness temperatures with a swath width of 1445 km and a horizontal resolution that varies from 6 km (at 89 GHz) to 60 km (at 6.9 GHz). The TMI instrument is aboard the TRMM mission since November 1997 and measures the intensity of radiation at five separate frequencies: 10.7, 19.4, 21.3, 37, 85.5 GHz. The TRMM orbit altitude is close to 400 km. As a consequence, TMI has a 760 km wide swath width with a high and variable horizontal resolution (6 km at 85.5 GHz to 50 km at 10.7 GHz) and also with an observation zenith angle ranging from about 47^o to 53^o.

In order to prepare the assimilation of SSMI/S observations over land, land surface emissivities have been calculated using observations from SSMI/S channels for which the contribution of the surface is strong enough (the so-called window channels). To evaluate SSMI/S land emissivities, many studies have been made and have involved land surface emissivity comparisons with emissivity estimates from other microwave sensors. The land emissivity variation with surface type and with frequency has also been studied. The inter sensor land emissivity comparison has been made using window channels from SSM/I, TMI and AMSR-E. Table 2 gives a list of all window channels used in this study.

Table 2: Window channels from microwave sensors

Channels	Frequency (GHz)	polarisation
SSMI/S		
1	50	V
12	19.35	H
13	19.35	V
14	22.2	V
15	37	H
16	37	V
17	91	H
18	91	H
SSM/I		
1	19.35	V
2	19.35	H
3	22.235	V
4	37.0	V
5	37.0	H
6	85.0	V
7	85.0	H
AMSRE		
1	6.9	V
2	6.9	H
3	10.65	V
4	10.65	H
5	18.7	V
6	18.7	H
7	23.8	V
8	23.8	H
9	36.5	V
10	36.5	H
TMI		
1	10.65	V
2	10.65	H
3	19.35	V
4	19.35	H
5	21.3	V
6	37.0	V
7	37.0	H
8	85.5	V
9	85.5	H

2.2 Land surface emissivity estimations

For a non scattering plane-parallel atmosphere, assuming a flat and specular surface and for a given zenith angle and frequency, the brightness temperatures (noted Tb, hereafter) observed by the sensor can be expressed as:

$$T_b(\nu,\theta) = T_s\,\varepsilon(\nu,\theta)\,\Gamma + (1-\varepsilon(\nu,\theta))\,\Gamma\,T_a^{\downarrow}(\nu,\theta) + T_a^{\uparrow}(\nu,\theta) \tag{1}$$

$$\Gamma = \exp\left(\frac{-\tau(0,H)}{\cos(\theta)}\right) \tag{2}$$

where $T_b(\nu,\theta)$ and $\varepsilon(\nu,\theta)$ represent the Tb measured by the sensor and the surface emissivity at frequency ν and at observation zenith angle θ respectively. T_s, $T_a^{\downarrow}(\nu,\theta)$, and $T_a^{\uparrow}(\nu,\theta)$ are the skin temperature, the atmospheric down-welling and upwelling Tbs respectively. Γ is the net atmospheric transmissivity and can be expressed as a function of the atmospheric opacity $\tau(0,H)$ and the observation zenith angle θ. H is the top of atmosphere height.

The microwave land emissivity can then be retrieved as follows.

$$\varepsilon(\nu,\theta) = \frac{T_b(\nu,\theta) - T_a^{\uparrow}(\nu,\theta) - T_a^{\downarrow}(\nu,\theta)\,\Gamma}{(T_s - T_a^{\downarrow}(\nu,\theta))\,\Gamma} \tag{3}$$

Short-range forecast data (temperature / humidity profiles) are used as inputs to the radiative transfer model RTTOV ((5), (24), (16)) in order to calculate the atmospheric contribution to the measured Tb ($T_a^{\downarrow}(\nu,\theta)$, $T_a^{\uparrow}(\nu,\theta)$,$\Gamma$). The surface temperature is taken from the short-range forecasts.
Many authors have previously used such a method to estimate the land surface emissivity using satellite observations : see for instance studies of (10), (6), (12), (18), (20), (21), (15), among many others.

2.3 Technical modifications to the assimilation system and evaluation with SSM/I

For simplification sake, 4D-CLEAR and 4D-CLOUDY will connote assimilation framework in which microwave observations are assimilated in 4D-VAR under clear and cloudy situations respectively. By April 2008 (first visit), only SSM/I observations were allowed for processing in the 4D-CLOUDY system and were then used instead of SSMI/S. Few months later, observations from SSMI/S, TMI and AMSR-E have been allowed into the 4D-CLOUDY system (second visit in November 2008).

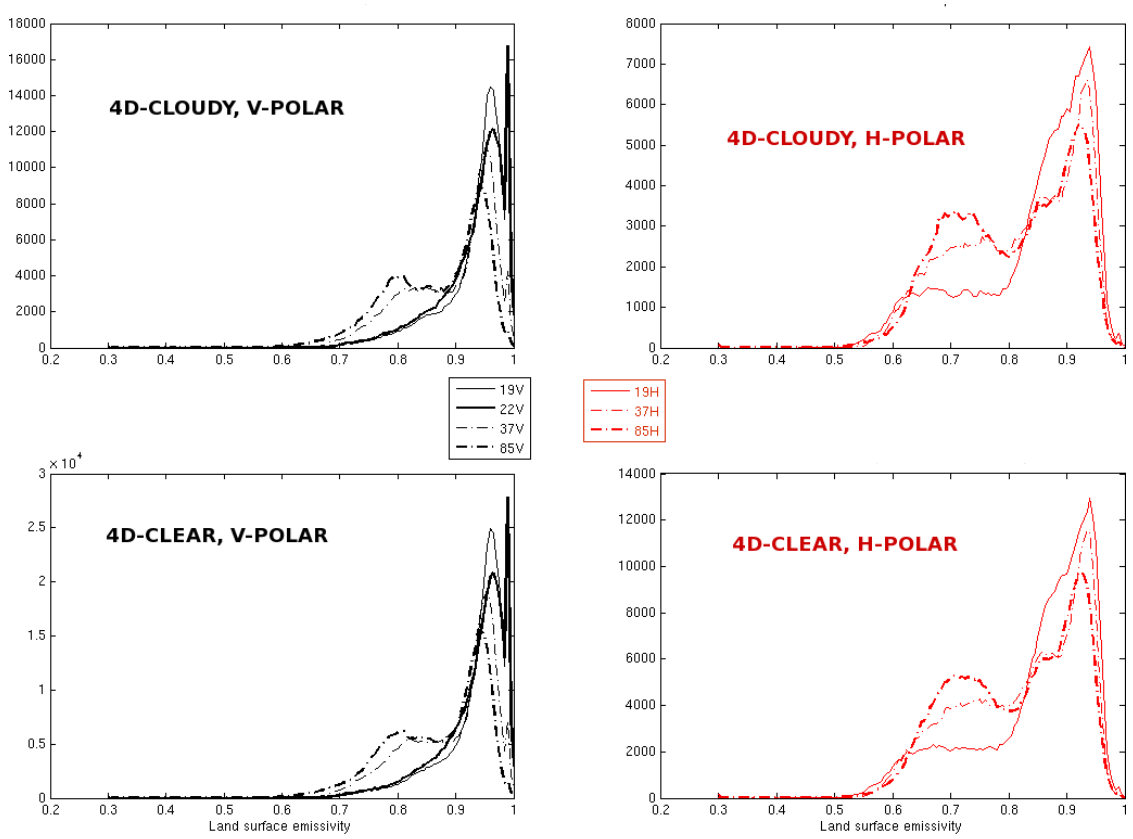

Figure 2: Histograms of land emissivities obtained from the 4D-CLEAR (subplots c, d) and 4D-CLOUDY (subplots a, b) systems and for SSM/I channels. Red lines are for channels with a horizontal polarization whereas black lines are for channels with a vertical polarization. The histograms have been computed at a global scale and using two weeks of data.

During the first visit, we have started emissivity developments using SSM/I observations only. We were then able to extend our development to SSMI/S, TMI and AMSR-E during the second part of the visit in November. The land emissivity calculation module has been first developed in the ARPEGE assimilation system in order to assimilate more AMSU-A and AMSU-B sounding channels over land and under clear sky situations (13). Then, the module's routines have been implemented within IFS and adapted to retrieve the land emissivities using clear sky SSMI/S observations (14). However, several technical modifications to the emissivity module's routines were required in order to retrieve the land emissivity from cloudy obser-

vations. In fact, cloudy and clear microwave radiances are separately processed within the 4D-VAR. Consequently, the clear-sky emissivity computation module, which has been previously developed for 4D-CLEAR, could not be used for cloudy observations. A new interface to the radiative transfer module has been added to 4D-CLOUDY together with appropriate new routines to allow this retrieval, the backup copy and the use of land emissivities within the system. The new interface has been developed to easily handle observations from different sensors, including SSM/I and SSMI/S. To evaluate the new emissivity module (within 4D-CLOUDY), comparisons have been made using SSM/I data. Land surface SSM/I emissivities retrieved from 4D-CLOUDY have been compared with SSM/I emissivities from 4D-CLEAR over a two-week period (from the 11th to 24th of March 2008). The obtained emissivity maps at all SSM/I frequencies (averaged over two weeks, not shown) from 4D-CLEAR and 4D-CLOUDY have been found to be in very good agreement. Figure 2 shows SSM/I emissivity histograms from 4D-CLEAR and 4D-CLOUDY at 7 channels. Red curves are for SSM/I channels with a horizontal polarization whereas black curves are for SSM/I channels with a vertical polarization. The histograms have been computed at a global scale and using two weeks of data. A very good agreement between 4D-CLEAR and 4D-CLOUDY emissivities can be noticed. We should note that we have many more emissivity estimates from 4D-CLEAR than from 4D-CLOUDY. This is due to the fact that, in many cases, observations are rejected in 4D-CLOUDY, including the case when the surface temperature is below a fixed threshold.

3 Towards the assimilation of SSMI/S over land

3.1 Evaluation of SSMI/S land surface emissivities

Land surface emissivities have been derived within the CLOUDY-4D system using 3 weeks (from 01/08/2007 to 20/08/2007) of observations from many sensors including SSMI/S. The retrieval has been performed at window channels as they appear in Table 2. The inter-sensor emissivity comparison is a good way to check the consistency of SSMI/S retrieved emissivities, in terms of spatial, temporal and frequency variations. Such a comparison will also be very important to check the calibration of SSMI/S window channels. It should be mentioned here that emissivities derived from satellite observations are in fact "effective emissivities" because they are integrated over the satellite foot print. Ideally, satellite emissivities should be compared with some independent emissivity measurements. However, such in-

dependent measurements are not available and inter-sensor emissivity comparisons have been performed instead.

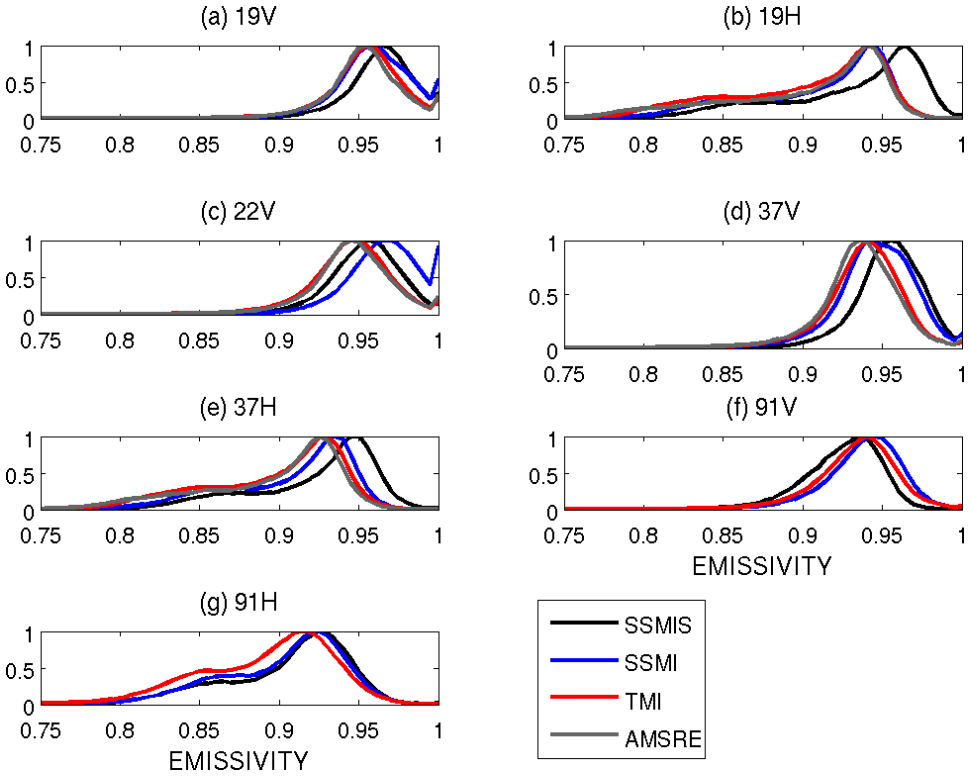

Figure 3: Normalised histograms of land emissivity of seven SSMI/S channels surface channels: (a) 19V, (b) 19H, (c), 22V, (d) 37V, (e) 37H, (f) 85V and (g) 85H. When possible, land emissivity histograms from SSM/I, AMSRE and TMI are presented. Results are for 3 weeks and for latitudes ranging from -30 to +30 degrees (to match TMI coverage).

Figure 3 shows land emissivity normalised histograms at seven SSMI/S frequencies: (a) 19V, (b) 19H, (c), 22V, (d) 37V, (e) 37H, (f) 85V and (g) 85H. For each frequency and whenever it is possible, normalised emissivity histograms from the closest (in frequency) AMSR-E, TMI and SSM/I channel are plotted.

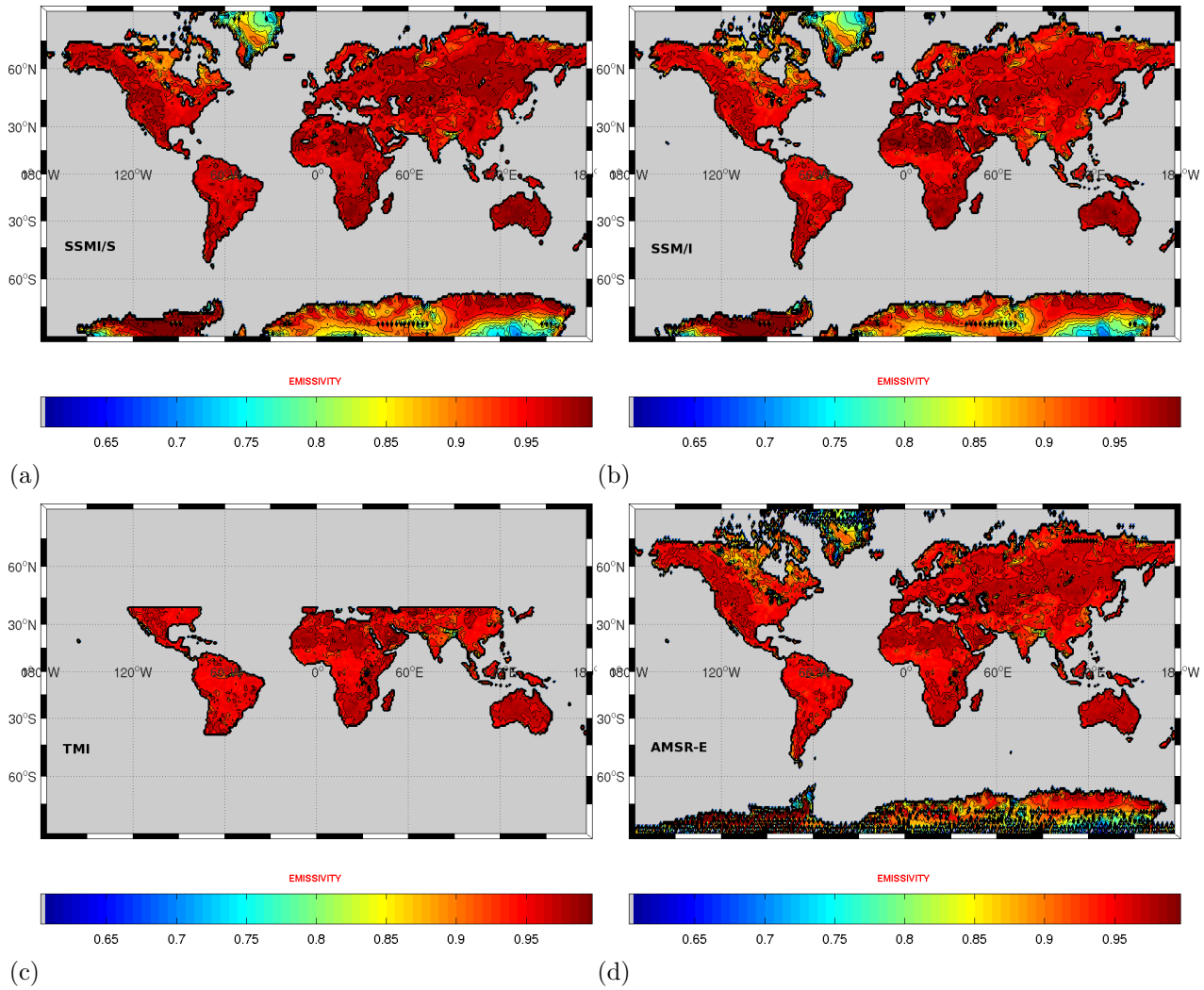

Figure 4: Mean land emissivity maps averaged over a 3 week period (from 2007-08-01 to 2007-08-20) and derived using observations from 19 GHz vertical polarisation from (a) SSMI/S (b) SSM/I, (c) TMI and (d) AMSR-E.

To make comparisons with TMI emissivities, only data located within $\pm$ 30 degrees of latitudes have been used for these plots. One should notice the rather good agreement between SSMI/S emissivities and emissivities coming from other sensors. SSMI/S 19H emissivities appear however systematically larger than emissivities from other sensors. This point is being investigated. Figure 4 shows mean emissivity maps at 19 GHz at vertical polarization and obtained using measurements from

(a) SSMI/S, (b) SSM/I, (c) TMI and (d) AMSR-E. Once again, one should notice the very good agreement between emissivities from all sensors including SSMI/S. The emissivity maps show the expected variations with surface types: contrarily to forests, desert and snow areas exhibit low emissivity values and high emissivity differences (between vertical and horizontal polarisations).

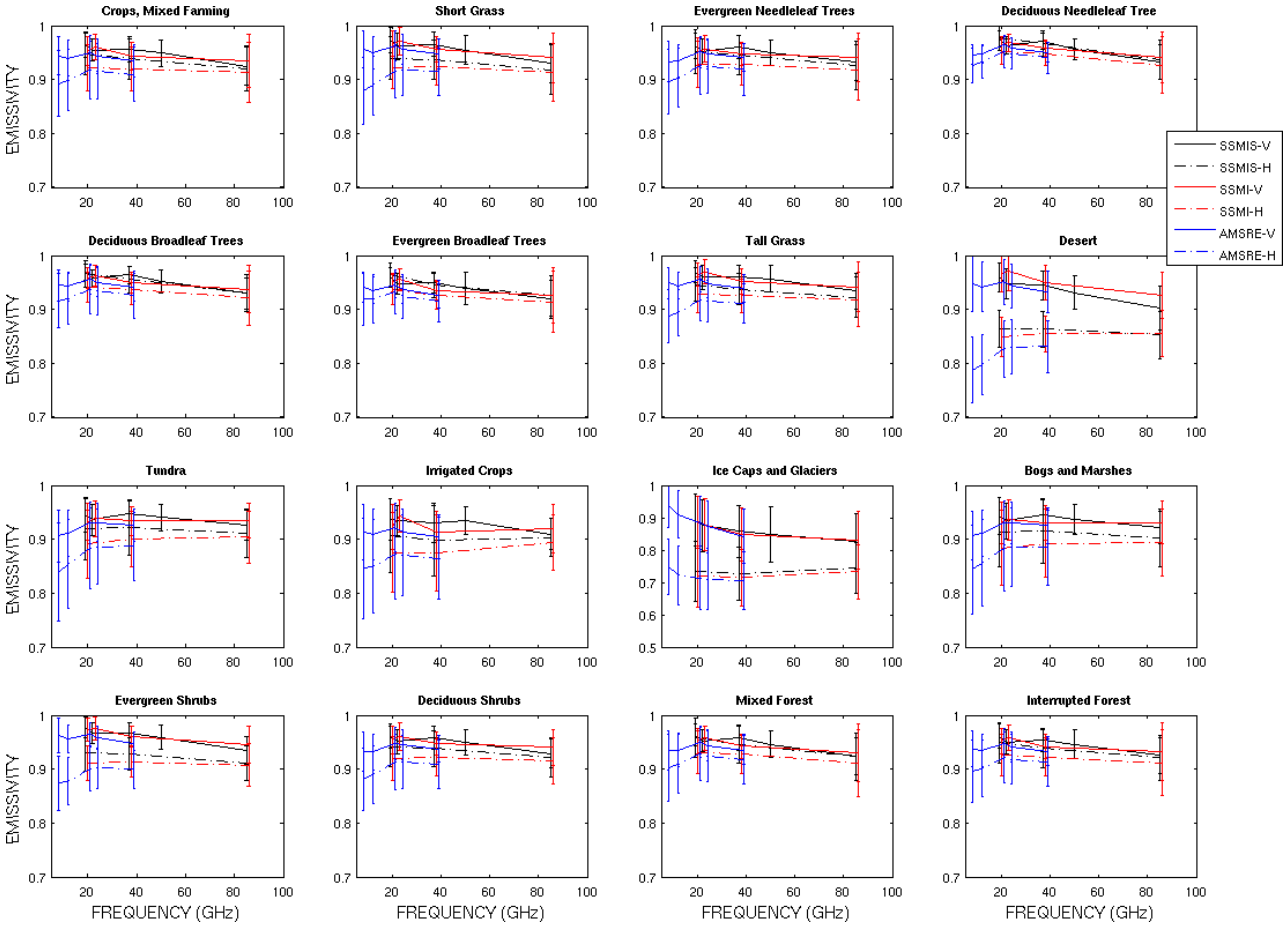

Figure 5: errorbars describing the land emissivity variation with frequency and with respect to 16 surface types (from the BATS climatology). Results are for a three week period and for SSMI/S (in black), SSM/I (in red) and AMSR-E (in blue). Frequencies with vertical polarisation (solid lines) have been separated from frequencies with horizontal polarisation (dashed lines)

Lakes and rivers are also associated with low emissivities. Besides the emissiv-

ity variation in space, the frequency dependency of the SSMI/S emissivities have also been studied. For this task we have used The Biosphere-Atmosphere Transfer Scheme (BATS) datasets to identify 16 surface types (7). Figure 5 shows, for a given surface type, errorbars which describe the variation of emissivity with respect to the frequency. Mean emissivities coming from SSM/I and AMSRE have been added to the plots. The agreement between emissivity curves is very good. The SSMI/S emissivity seem to vary smoothly with frequency, which is coherent with previous finding.

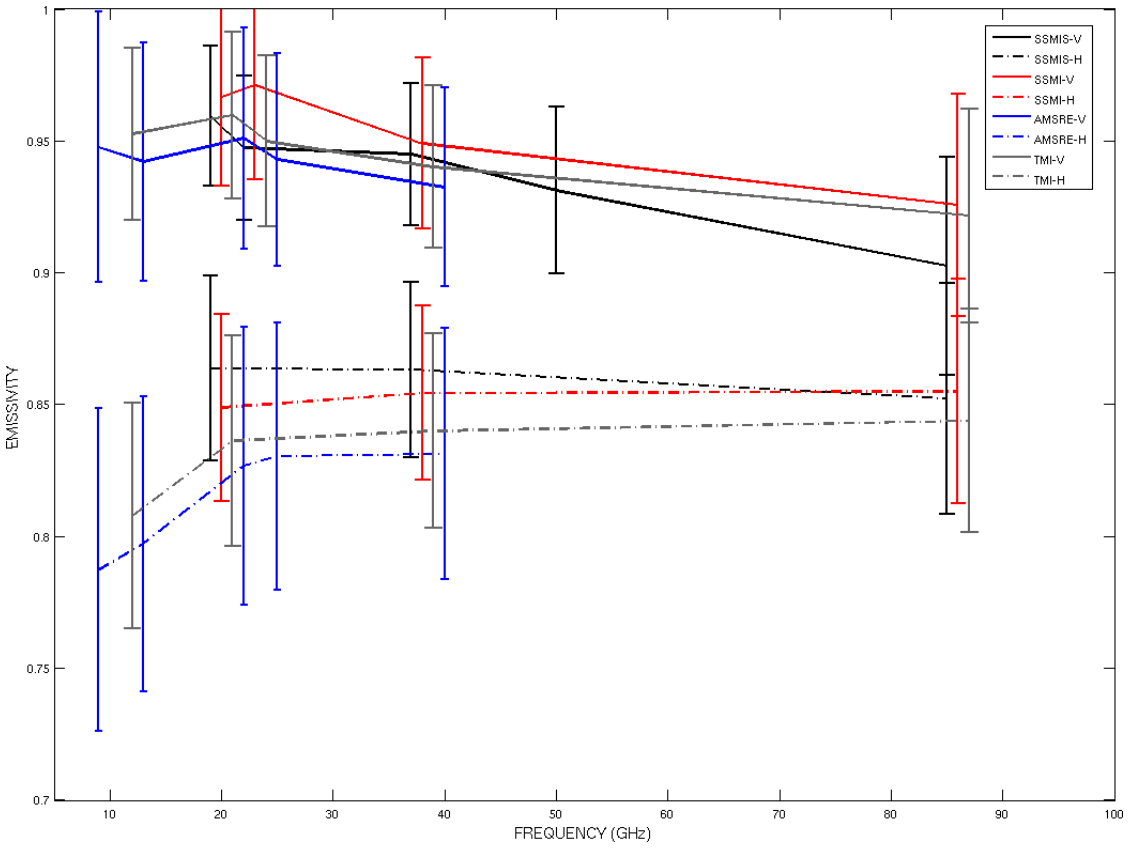

Figure 6: errorbars of the land emissivity variation with frequency and over desert surface type. Results are for a three week period and for SSMI/S (in black), SSM/I (in red), AMSR-E (in blue) and TMI (in grey). Frequencies with vertical polarisation (solid lines) have been separated from frequencies with horizontal polarisation (dashed lines).

For a given observation frequency, as it was expected, the emissivity differences between vertical and horizontal over forest are negligeable and rather large over desert and Ice Glaciers. At microwave frequencies, forests behave like a black body and no differences are expected from measurement at vertical and horizontal polarisations. Deserts are usually associated with lower emissivities with respect to forests. In fact, deserts combine effects of high dielectric constant of some rock materials (25) as well as complex scattering effects (11). Figure 6 shows the frequency variation of SSMI/S emissivities over desert. The spectral variation curves of SSM/I, AMSR-E and TMI are also presented in this figure.

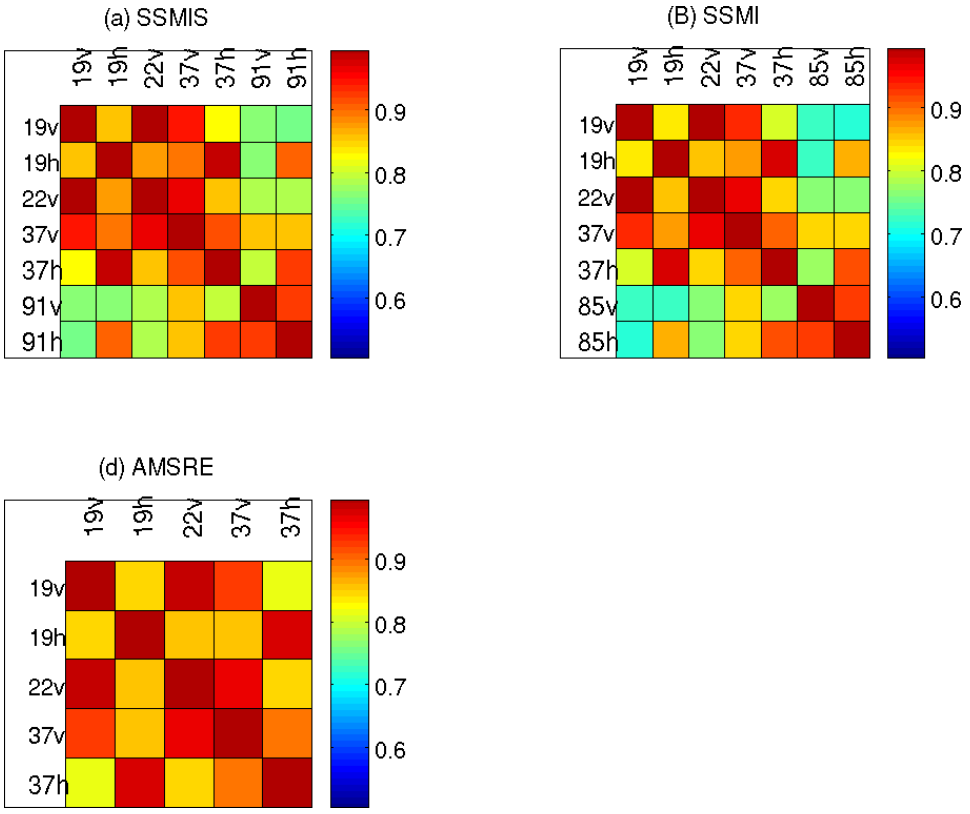

Figure 7: Land surface emissivity correlation coefficients obtained using surface channels from (a) SSMI/S, (b) SSM/I and (c) AMSRE. The correlations have been calculated over the glob and using three weeks of data.

As expected, large differences can been seen between emissivities at vertical and horizontal polarisations. For vertical and for horizontal polarisations, a very

good agreement can be noticed between all sensors. At vertical polarisation, the land emissivity tends to decrease with increasing frequencies. On the other hand, emissivities at horizontal polarisation, seem to increase with increasing frequencies. The emissivity correlation coefficients have also been determined for SSMI/S, SSM/I and AMSR-E surface channels (see Figure 7) using 3 weeks of global data. We noticed a rather good agreement between emissivity correlation coefficients from SSMI/S, SSM/I and AMSR-E. The agreement is best between SSMI/S and AMSR-E emissivities. Land surface SSMI/S emissivities will be further analysed in order to check their seasonal variations. Such analysis will requires the computation of land emissivities over one year at least.

3.2 Observation operator performances

SSMI/S Tbs over land have been simulated using the RTTOV-SCATT radiative transfer model for three weeks of data and for a selection of temperature (channels 2 to 5) and humidity channels (channels 8 to 11). A good knowledge of surface emissivity is beneficial to sounding channels (temperature and humidity) that receive a weaker contribution from the surface. Over land, the surface emissivity has been derived at 50V GHz (channel 1) and at 91H GHz (channel 18) and has been given to temperature and to humidity channels respectively. Over sea, the FASTEM model (9) has been used to estimate sea surface emissivities. The differences between observed and simulated radiances using the background fields (called 'fg-departures' hereafter) have been computed. Histograms of fg-departures obtained globally and for SSMI/S temperature and humidity channels are given in Figure 8. Land and sea histograms as well as temperature and humidity channel histograms have been plotted separately. No bias corrections have been applied for these comparisons. The results shown in Figure 8 indicate that fg-departure statistics are as good over land as they are over sea. Some large biases can be seen for fg-departure histograms at 150 GHz (positive fg-departures) partly reflecting larger biases over Antartica and FASTEM biases over sea at 91H GHz. But overall, the fg-departure statistics are rather satisfactory. The fg-departure statistics are further evaluated in Figure 9. Subplot Figure 9.a and Figure 9.c show mean global bias and standard deviation maps for SSMI/S channel 2 (52.3 GHz) fg-departures. Subplot Figure 9.b and Figure 9.d show mean global bias and standard deviation maps for SSMI/S channel 9 (183±6 GHz) fg-departures. One should notice the rather low fg-departure biases over land: no specific features could be seen over land compared with sea (see 9.a). Some positive biases can be noticed over land and over sea which are mainly due to the presence of clouds. This result is very important since it reflects our ability

to detect and then assimilate cloud affected observations over sea and over land from this channel. Similar conclusions can be made regarding results from channel 9. The fg-departures standard deviations are also acceptable, they are larger in the Tropics where the cloud contamination is likely to occur. These results are very encouraging and suggest that it is possible to assimilate SSMI/S temperature and humidity channels over land and under cloudy/rainy situations.

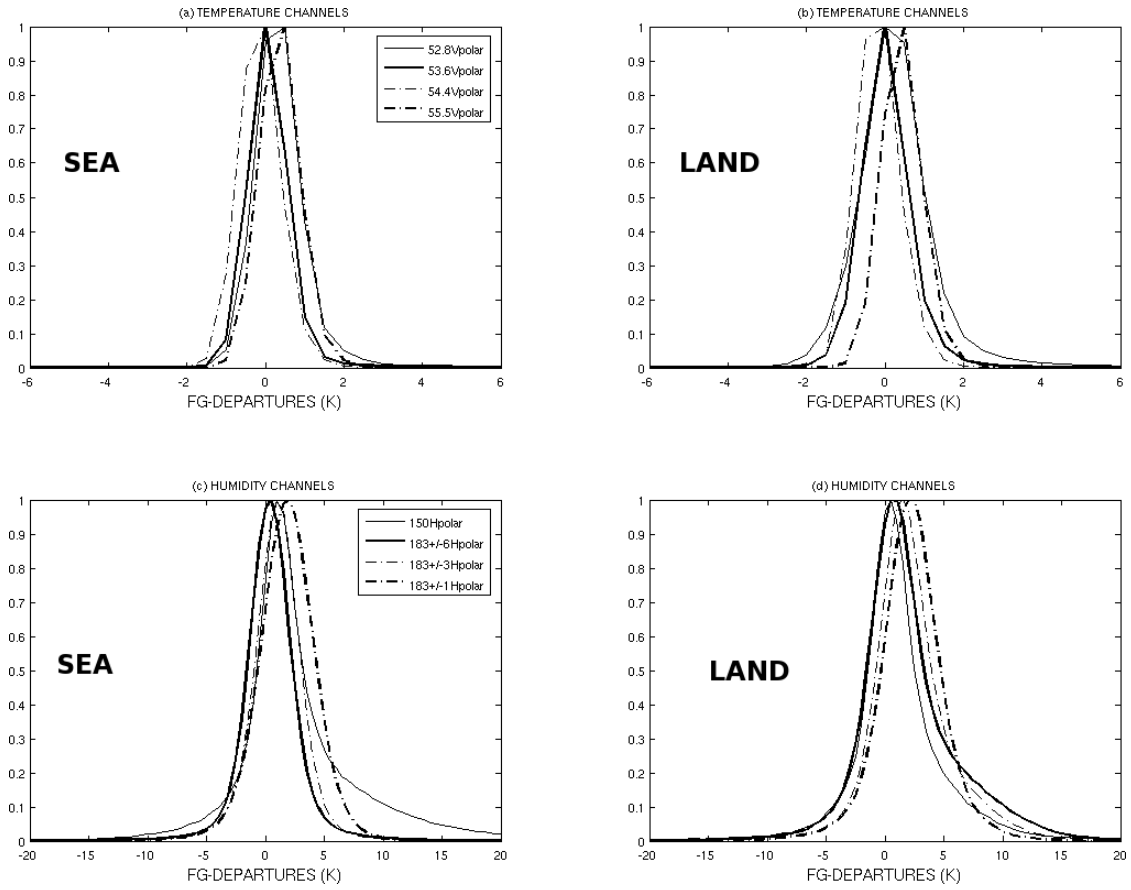

Figure 8: Histograms of fg-departures (without bias correction) obtained globally and for SSMI/S temperature (channels 2 to 5) and humidity channels (channels 8 to 11). Results are for a three week period and have been separated for sea and land. Over land, temperature and humidity channels have been given the emissivity estimated at 50 GHz (channel 1) and the emissivity estimated at 91H (channel 18) respectively. Over sea, FASTEM emissivities have been used.

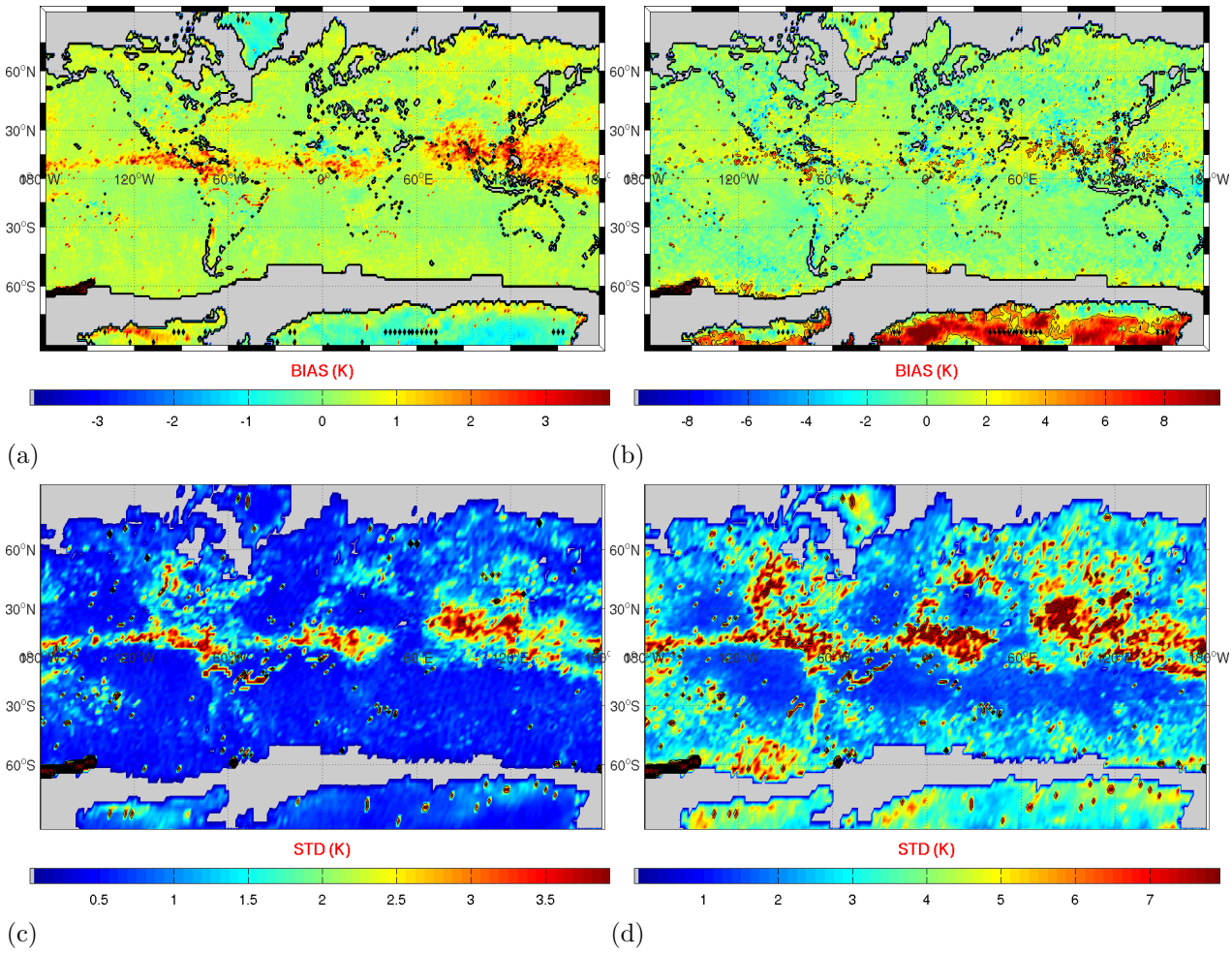

Figure 9: Subplots (a) and (b): Mean fg-departure biases at SSMI/S 52.3V GHz and at SSMI/S 183±6H GHz respectively; Subplots (c) and (d) are for fg-departure standard deviations at SSMI/S 183±6H GHz respectively. The statistics have been made using three weeks of data. Over land, temperature and humidity channels have been given the emissivity estimated at 50 GHz (channel 1) and the emissivity estimated at 91H (channel 18) respectively. Over sea, FASTEM emissivities have been used.

4 Discussion and conclusions

This work reports on some feasibility studies conducted at ECMWF in order to prepare the assimilation of SSMI/S observations over land and under cloudy situations. Several land emissivity developments have been undertaken to allow the land emissivity estimation within the 4D-CLOUDY system at ECMWF. Land emissivities at seven SSMI/S frequencies have been calculated and their consistency, in terms of spatial, temporal and spectral variations has been checked. Inter-sensor emissivity comparisons have been made by comparing SSMI/S emissivities with emissivities derived from SSM/I, AMSR-E and TMI observations. It has been shown that SSMI/S emissivities are rather in good agreement with emissivities from the other three sensors. A slight positive bias was observed for SSMI/S emissivities at 19H with respect to the other sensors. Land SSMI/S Tbs from a selection of temperature and humidity have been simulated using the RTTOV-SCAT model. Land surface emissivities calculated at two selected window channels have been given to the sounding channels. The Tbs simulations have been found to be in a very good agreement with observations. Moreover, fg-departures (observations - simulations) have been found as good over land as they are over sea. The fg-departure analyses have shown that it is possible to take advantage of the information content of SSMI/S sounding channels under cloudy situations when the land surface emissivity is accurately described. Assimilation experiments are already planned to check the impact of SSMI/S channels in the ECMWF 4D-VAR system. At least four assimilation experiments will be run:

1. the first one assimilating SSMI/S temperature channels over sea;
2. the second experiment assimilating SSMI/S temperature channels over sea and over land;
3. the third one assimilating SSMI/S temperature and humidity channels over sea;
4. the fourth experiment assimilating SSMI/S temperature and humidity channels over sea and over land;

References

[1] P. Bauer, P. Lopez, A. Benedetti, D. Salmond, M. Bonazzola and S. Saarinen,2006a,Implementation of 1D+4D-Var Assimilation of Microwave Radiances

in Precipitation at ECMWF, Part II: 4D-Var,*Q. J. R. Meteorol. Soc*, 620,2277-2306

[2] P. Bauer, P. Lopez, A. Benedetti, D. Salmond, M. Bonazzola and S. Saarinen,2006b,Implementation of 1D+4D-Var Assimilation of Microwave Radiances in Precipitation at ECMWF, Part I: 1D-Var, *Q. J. R. Meteorol. Soc*, 620, 2307-2332

[3] W. Bell, S. English, B. Candy, N. Atkinson, F. Hilton, S. Swadley, B. Campbell, N. Bormann, G. Kelly and M. Kazumori, 2008, The assimilation of SSMI/S radiances in numerical weather prediction models, *IEEE Trans. On Geoscience and Remote sensing*, 46, 4, Part 1, pages 884-900

[4] W. Bell, S. English, B. Candy, F. Hilton, S. Swadley, G. Kelly, 2006, An Initial Evaluation of SSMIS Radiances for Radiance Assimilation Applications, *Microrad*, SanJuan.

[5] J. Eyre, 1991, A fast radiative transfer model for satellite sounding systems, *ECMWF Tech. Memo.*, 176, 28 pp., Availabale from ECMWF, Shinfield Park, Reading Berkshire RG2 9AX, UK

[6] B. J. Choudhury, 1993, Reflectivities of selected land surface types at 19 and 37 GHz from SSM/I observations, *Remote Sens. Environ*, 46, pages 1-17.

[7] R. E. Dickinson, A. Henderson-Sellers, P. J. Kennedy, and M. F.Wilson, 1986, Biosphere-Atmosphere Transfer Scheme (BATS) for the NCAR Community Climate Model, Boulder, CO.

[8] C. O'Dell and P. Bauer, 2007, Assimilation of precipitation-affected SSMIS radiances over land in the ECMWF data assimilation system, *SAF-HYDROLOGY final Tech. Rep.*

[9] English S. J., and T. J. Hewison, 1998: A fast generic millimeter-wave emissivity model. *Microwave Remote Sensing of the Atmosphere and Environment, T. Hayasaka et al., Eds., International Society for Optical Engineering (SPIE Proceedings Vol. 3503)*, 288-300.

[10] G. W. Felde and J. D. Pickle, 1995, Retrieval of 91 and 150 GHz Earth surface emissivities, *J. Geophys. Res.*, 100, D10, pages 20855-20866

[11] N. C. Grody and F. Weng, 2008, Microwave Emission and Scattering From Deserts: Theory Compared With Satellite Measurements, *IEEE Trans. On Geoscience and Remote sensing*, 46, Issue2, pages 361-375.

[12] A. S. Jones and T. H. Vonder Haar, 1997, Retrieval of microwave surface emittance over land using coincident microwave and infrared satellite measurements, *J. Geophys. Res*, 102, D12, pages 13609-13626

[13] F. Karbou, E. Gérard and F. Rabier, 2006, Microwave land emissivity and skin temperature for AMSU-A and -B assimilation over land, *Q. J. R. Meteorol. Soc*, 620, 2333-2355(23)

[14] F. Karbou, N. Bormann and J-N. Thépaut, 2007, Towards the assimilation of satellite microwave observations over land: feasibility studies using SSMI/S, AMSU-A and AMSU-B, *NWPSAF Tech. Rep.*, 37pp

[15] F. Karbou, C. Prigent, L. Eymard and J. Pardo, 2005, Microwave land emissivity calculations using AMSU-A and AMSU-B measurements, *IEEE Trans. on Geoscience and Remote Sensing*, 43, 5, 948-959.

[16] M. Matricardi, F. Chevallier, G. Kelly and J.N. Thépaut, 2004, Channel selection method for IASI radiances, *Q. J. R. Meteorol. Soc.*, 130, pages 153-173

[17] C. Mätzler, 1994, Passive microwave signatures of landscapes in winter, *Meteorol. Atmos. Phys*, 54, pages 241-260

[18] J.C. Morland, I. David, F. Grimes and G. Dugdale and T. J. Hewison, 2000, The Estimation of Land Surface Emissivities at 24 GHz to 157 GHz Using Remotely Sensed Aircraft Data, *Remote Sens. Environ.*, 73, pages 3323-3336

[19] J.C. Morland, I. David, F. Grimes and and T. J. Hewison, 2001, Satellite observations of the microwave emissivity of a semi-arid land surface, *Remote Sens. Environ.*, 77, pages 2149-2164

[20] C. Prigent and W. B. Rossow and E. Matthews, 1997, Microwave land surface emissivities estimated from SSM/I observations, *J. Geophys. Res.*, 102, pages21867-21890

[21] C. Prigent and J.P. Wigneron and B. Rossow and J. R. Pardo, 2000, Frequency and angular variations of land surface microwave emissivities: can we estimate SSM/T and AMSU emissivities from SSM/I emissivities?, *IEEE trans. Geosci. Remote Sensing.*, 38, pages 5, 2373-2386

[22] C. Prigent, F. Chevallier, F. Karbou, P. Bauer and G. Kelly, 2005, AMSU-A surface emissivities for numerical weather prediction assimilation schemes, *J. Applied Meteorology*, 44, pages 416-426

[23] B. Yan and F. Weng, 2008, Intercalibration Between Special Sensor Microwave Imager/Sounder and Special Sensor Microwave Imager, *IEEE trans. Geosci. Remote Sensing.*, 46, Issue 4, Part 1, pages 984-995

[24] R. W. Saunders, M. Matricardi and P. Brunel, 1999, An improved fast radiative transfer model for assimilation of satellite radiance observations, *Q. J. R. Meteorol. Soc.*, vol. 125, pages 1407-1425

[25] Ulaby, F. T., R. K. Moore, and A. K. Fung, 1986, Microwave Remote Sensing Active and Passive, Vol. 3, From Theory to Applications, *Addison-Wesley Publishing Co.*, 1097pp.